Accepted Manuscript

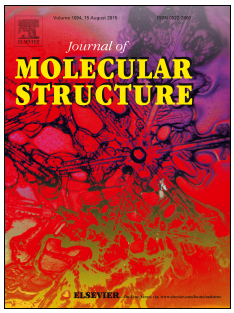

Structural investigation, spectroscopic and energy level studies of Schiff base: 2-[(3′-*N*-salicylidenephenyl)benzimidazole] using experimental and DFT methods

G.R. Suman, S.G. Bubbly, S.B. Gudennavar, S. Muthu, B. Roopashree, V. Gayatri, N.M. Nanje Gowda

PII: S0022-2860(17)30304-6

DOI: 10.1016/j.molstruc.2017.03.043

Reference: MOLSTR 23539

To appear in: *Journal of Molecular Structure*

Received Date: 11 September 2016

Revised Date: 5 March 2017

Accepted Date: 8 March 2017

Please cite this article as: G.R. Suman, S.G. Bubbly, S.B. Gudennavar, S. Muthu, B. Roopashree, V. Gayatri, N.M. Nanje Gowda, Structural investigation, spectroscopic and energy level studies of Schiff base: 2-[(3′-*N*-salicylidenephenyl)benzimidazole] using experimental and DFT methods, *Journal of Molecular Structure* (2017), doi: 10.1016/j.molstruc.2017.03.043.

Structural Investigation, Spectroscopic and Energy Level Studies of Schiff base: 2-[(3′-N-salicylidenephenyl)benzimidazole] using Experimental and DFT methods.

G. R. Suman[a], S. G. Bubbly[a,*], S. B. Gudennavar[a], S. Muthu[b], B. Roopashree[c], V. Gayatri[c] and N. M. Nanje Gowda[d]

[a]*Department of Physics, Christ University, Bengaluru -560 029.*
bDepartment of physics. Aringer Anna Govt. Arts college. Cheyyar. Tamilnadu. India-604407.
[c]*Department of Chemistry, Central College Campus, Bangalore University, Bengaluru -560 001.*
[d]*Department of Chemistry, Christ University, Bengaluru-560 029.*

*Corresponding e-mail: bubbly.sg@christuniversity.in

Abstract: The Schiff base 2-[(3′-N-salicylidenephenyl)benzimidazole] (Spbzl) was characterized by FT-Raman, ^{1}H NMR, ^{13}C NMR and single crystal X-ray diffraction technique. Crystallographic studies reveal the presence of two water molecules in the asymmetry unit which aid the intermolecular hydrogen bonding with imidazole ring, and the trans-conformation of the azomethine bond. Theoretical computations conducted using density functional theory (DFT) analysis support the experimental facts. Energy levels estimated by DFT studies are in good agreement with the values obtained from cyclic voltammetry technique. Frontier molecular orbital analysis shows that charge transfer has taken place from donor to acceptor moiety, which is also supported by the high hyperpolarizability values in both gaseous and solution phases, indicating high charge transfer capability of the molecule. A comparative theoretical study of Spbzl with derivative 4-((3-(1H-benzimidazol-2-yl)phenylimino)methyl)-3-hydroxybenzoic acid (Pbzlb) having an added anchor group COOH substituted at para position in the acceptor ring has been made. The result shows the feasibility of charge transfer to the semiconductor surface in dye sensitized solar cell (DSSC) applications for Pbzlb.

Key words: Schiff base; Benzimidazole; NMR; Density functional theory; Dye sensitized solar cell.

1. Introduction

Benzimidazole is a potential molecular frame work in the development of compounds of pharmaceutical and biological interest for diverse receptors and also it has the ability to interact with various enzymes and receptors [1]. Benzimidazole derivatives are also used as fluorescent probes and fluorescent tags [2]. Owing to their high thermal stability, electron transporting ability and ease of synthesis [3, 4] as compared to π-bridge analogues like thiophene and ethenyl derivatives [5], they are utilized in the devising of organic light emitting diodes (OLED) and organic solar cells.

The conjugation of the benzimidazole ring with various aromatic aldehydes through –N=CH– group (Schiff base) has brought significant change in the behaviour of the overall ligand frame work [6]. Schiff base compounds exhibit good thermochromic and photochromic

properties [7-9]. Monomer Schiff bases have been used as dye sensitizers in solar cells due to their effective excited electron transferring ability [10-12]. Incorporation of Schiff base –N=CH– unit as a bridge in molecules could also increase the conjugation. Evaluation of the usefulness of such molecules for photovoltaic applications based on the investigations on charge transfer mechanism and energy level analysis has gained much research interest. Hence in the present work, we have investigated the molecular properties of 2-[(3′-N-salicylidenephenyl)benzimidazole] (Spbzl), a hybrid molecule of aminophenyl benzimidazole and salicylaldehyde conjugated through an azomethine linkage, using experimental and computational approaches.

Density functional theory (DFT) computations and electrochemical studies were used for the investigations on charge transfer properties and energy level analyses. Experimental observations of FT-IR, FT-Raman, UV-Visible [13], NMR and single crystal X-ray analysis were correlated with the theoretical computations carried out with Gaussian 09 package based on DFT using hybrid model B3LYP at 6-311G(d, p) level basis set [14]. Energy level analyses performed using both electrochemical studies and DFT computations were used to check the possibility of charge transfer from excited state of the dye to conduction band of the semiconductor across the dye-semiconductor interface. Interaction between electron donor and acceptor units was understood based on the value of stabilization energy, which was obtained using natural bonding orbital (NBO) theory. Anchoring groups like COOH play a crucial role in DSSC performance. It is reported that COOH position in para position is geometrically favorable to anchor on semiconductor and shows better efficiency compared to ortho and meta positions [15-17]. Hence properties of Spbzl were also compared with the computationally designed molecule having COOH anchoring unit at para position on the acceptor side (salicylidene). Fig. 1 shows the structure of 4-((3-(1H-benzimidazol-2-yl)phenylimino)methyl)-3-hydroxybenzoic acid (Pbzlb) which can be a reference for tuning of Spbzl for further DSSC studies.

Organic molecules exhibiting nonlinear optical (NLO) properties are gaining considerable importance, as they can serve as an alternative to inorganic materials. NLO properties such as mean polarizability, mean first hyperpolarizability and dipole moment were evaluated for Spbzl and Pbzlb in gas and solution (dichloromethane; DCM) phases using B3LYP/6-311G(d, p) and CAM-B3LYP functional. Prompted by the high value of mean first hyperpolarizability from DFT computations, we measured the second harmonic generation (SHG) efficiency of Spbzl. The experimental SHG efficiency of Spbzl is less compared to KDP and urea.

2. Experimental

2.1 Spectroscopic and Crystal Structure Studies

The Schiff base 2-[(3′-N-salicylidenephenyl)benzimidazole] (Spbzl) was synthesized (Scheme 1) as reported elsewhere [13]. ^{1}H and ^{13}C NMR spectra were recorded on Bruker Av 400 MHz instrument using deuterated dimethyl sulfoxide (DMSO-d_6) and methanol (CD_3OD). The ^{1}H and ^{13}C NMR chemical shifts are reported as δ, in parts per million

relative to tetramethylsilane, as an internal reference, and coupling constants (J) in Hz. FT-IR and FT-Raman spectra were recorded using Nicolet NXR and Nicolet 6700 spectrometers respectively. Single crystal X-ray diffraction data were collected using Bruker Kappa Apex2 diffractometer with molybdenum Kα (λ=0.71073 Å) radiation at 293 K. The structure was solved by direct methods and refined by full matrix least-squares against F^2 using all data (SHELX97) [18]. Isotropic refinement of all hydrogen atoms and anisotropic refinement of all the non-hydrogen atoms converged the R-factor to 0.0412. Details of crystallographic experimental information are provided as supplementary material (STable 1).

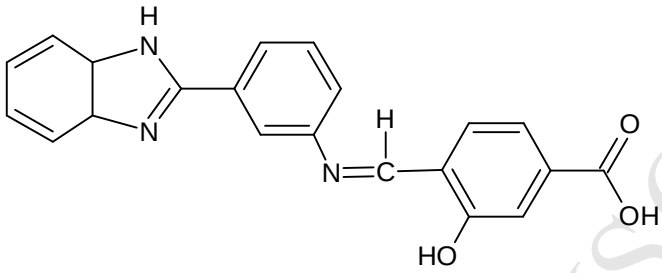

Fig. 1. Structure of 4-((3-(1H-benzimidazol-2-yl)phenylimino)methyl)-3-hydroxybenzoic acid (Pbzlb).

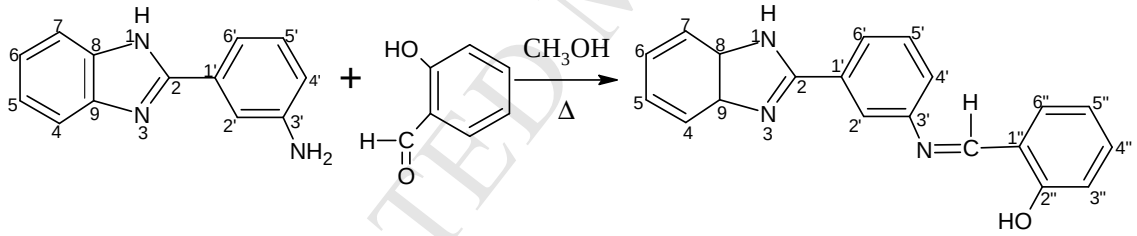

m-aminophenyl benzimidazole Salicylaldehyde 2-[(3′-N-salicylidenephenyl)benzimidazole]

Scheme 1

2.2. Photophysical and Electrochemical Measurements

UV-Visible absorption and fluorescence emission spectra of 10^{-5} M concentrations of Spbzl in N, N-dimethylformamide (DMF) were recorded using Hitachi U-3310 UV-VIS and Hitachi F-7000 fluorescence spectrophotometers respectively [19]. Electrochemical measurements were performed using CH instrument 660B work station at room temperature using glassy carbon (GC) as working electrode, platinum as counter electrode and silver wire as reference electrode. Cyclic voltammetry measurements were conducted at a scan speed of 0.1 V/s using ferrocene as standard. The potential values were recorded for 1 mM solute in DMF using 0.1 M tetrabutylammonium perchlorate (TBAP) as supporting electrolyte.

2.3. Quantum Chemical Studies

DFT computations were carried out using Gaussian 09 package [14]. The structure was optimized using Becke three-parameter (B3) [17], Lee-Yang-Parr (LYP) exchange-correlation function [18] and basis set 6-311G(d, p). FT-IR and FT-Raman simulated spectra were obtained using Gabedit software. In order to nullify the systematic error due to incompleteness in basis set a uniform scaling was done (scaling factor of 0.967) for B3LYP/6-311G(d, p) [21]. Inter and intra-molecular delocalization/hyper conjugation of the molecule were studied using NBO 3.1 program implemented in Gaussian 09. Electronic absorption spectra of Spbzl and Pbzlb in DMF were obtained using B3LYP/6-311G(d, p) method with polarizable continuum model (PCM) for solvent interaction. The NLO properties were also evaluated. The long-range corrected functional CAM-B3LYP which accounts for the electron exchange by combining both HF and hybrid functional was also used to obtain the excitation wavelength and NLO properties in both gaseous and solvent phases.

3. Results and Discussion

3.1 X-ray Structure Analysis

The X-ray crystallographic studies on Spbzl revealed the presence of two water molecules in the asymmetry unit (Fig. 2). The intra molecular charge transfer between N1 and C1 was evident from the bond distances of C1-O1, C6-C7, C1-C6, C6-C5 and C7=N1 (STable 2) and this was also supported by the high value of stabilization energy (58.24 kJ mol^{-1}) from π (C1-C6) (donor) to π* (C7-N1) (acceptor) calculated from NBO analysis using DFT (STable 3). The N3-C14 bond length of 1.328 Å suggests that it has partial double bond characteristics. The C8-N1-C7-C6 torsion angle [174.7(2)°] has revealed that the configuration around N1=C7 bond as *trans*- conformation, which is also supported by the DFT calculation [177.2(3)°]. A strong intra-molecular hydrogen bond O1-H1---N1 (Table 1) showed that the molecule was in phenol-imine form. The intermolecular interactions were aided by the O-H---O hydrogen bonding between the oxygen atoms of the water molecules, and N-H---O and O-H---N hydrogen bonds between oxygen atoms of water molecules and nitrogen atoms in the imidazole ring.

Spbzl was geometrically optimized and structural parameters were calculated using B3LYP/6-311G(d, p) method. The results (STable 2) were in agreement with the experimental values. The deviation in bond lengths and bond angles were due to the fact that the theoretical values were for the gaseous molecule and the experimental ones for Spbzl in solid state.

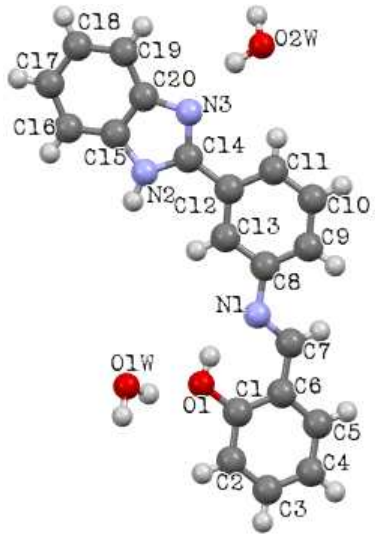

Fig. 2. ORTEP plot of the title compound.

Table 1
Intra and intermolecular hydrogen bonds

D- H...A	[ARU]	H...A (Å)	D...A (Å)	D -H...A (°)
O(1)-H(1)...N(1)	[1555.01]	1.81(2)	2.542(2)	148(3)
O(1W)-H(1W)...O(2W)	[2655.03]	1.81(2)	2.734(3)	165(3)
N(2)-H(2A)...O(1W)	[1455.02]	1.98(2)	2.895(2)	168(3)
O(1W)-H(2W)...O(1)	[1555.01]	1.86(2)	2.746(2)	155(3)
O(2W)-H(3W)...N(3)	[1555.01]	1.98(2)	2.895(2)	166(2)
O(2W)-H(4W)...O(1W)	[2545.02]	2.06(2)	2.939(3)	158(3)

[1455.00] = –1+x,y,z ; [2655.00] = 1–x,1/2+y,–z; [2545.00] = –x,–1/2+y,–z; [1555.01] = x, y, z.

3.2 Vibrational Spectroscopic Studies

Experimental and theoretical FT-IR and FT-Raman spectra are shown in Figs. 3 and 4 respectively. The experimental FT-IR and FT-Raman wave numbers along with those computed using DFT with B3LYP/6-311G(d, p) method and the potential energy distribution (PED) obtained using VEDA software are given in Table 2. The molecule contains 39 atoms and has 111 fundamental vibrations.

For Spbzl, the experimental FT-IR bands due to N-H, O-H and C-H stretching vibrations were observed in the range 3300-2850 cm^{-1} [23]. In the experimental FT-Raman νC-H was observed at 3061 and 2894 cm^{-1}. The theoretical νC-H was obtained at 3092 and 2933 cm^{-1} with PED values 90% and 99% respectively. The theoretical νN-H and νO-H were calculated to be 3545 and 3134 cm^{-1} respectively with PED contributions of 100% and 98%.

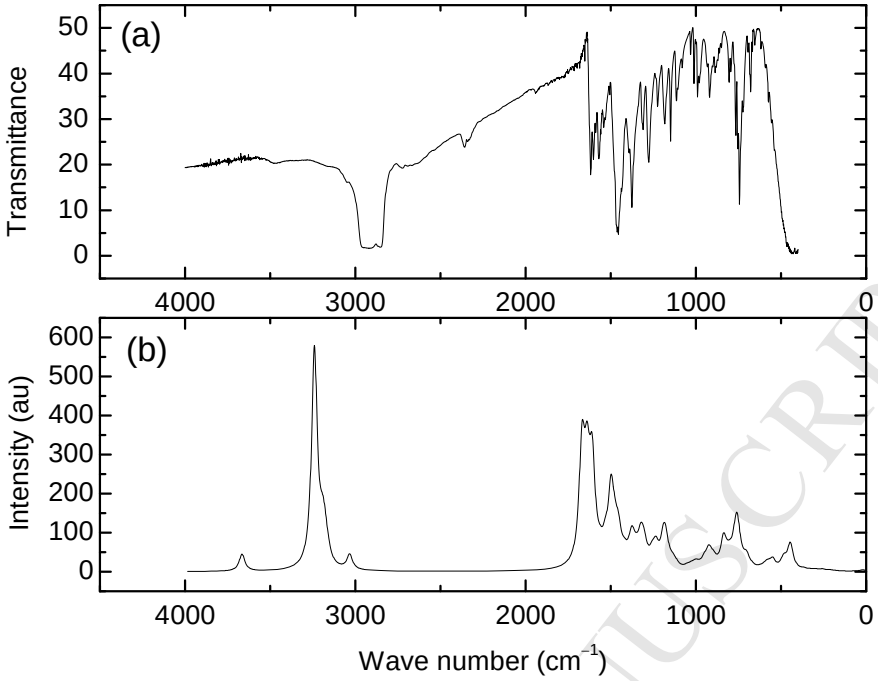

Fig. 3. FT-IR spectra of Spbzl (a) Experimental (b) Theoretical.

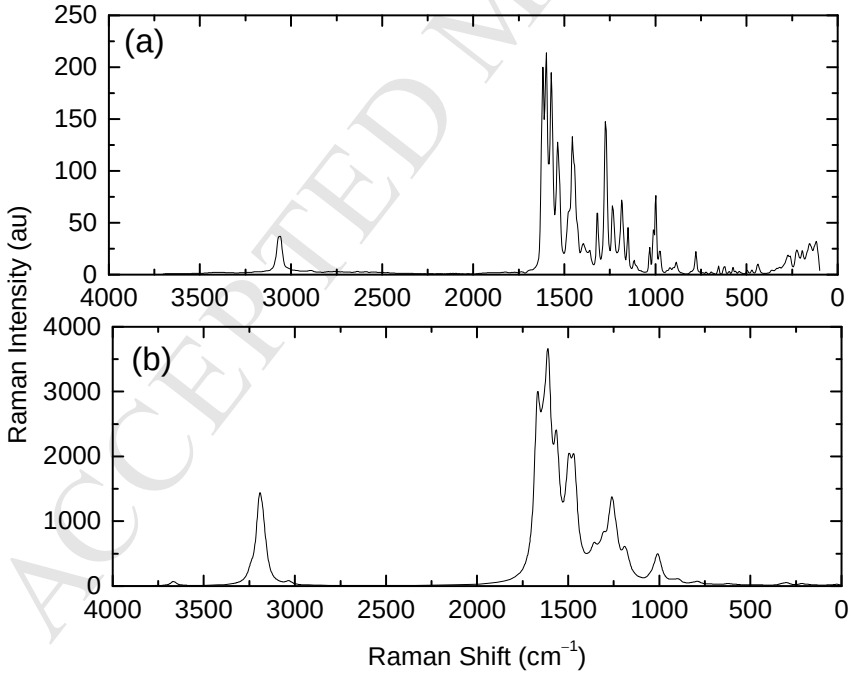

Fig. 4. Raman spectra of Spbzl (a) Experimental (b) Theoretical.

Experimental N-C stretching bands for Spbzl were observed both in FT-IR and FT-Raman at 1618, 1537 cm^{-1} and 1617, 1536 cm^{-1} respectively. The theoretical vibrations were at 1615 and 1556 cm^{-1} with PED contributions 30% and 10% respectively. Other vibrational frequencies are listed in Table 2.

Table 2

Experimental and theoretical FT-IR and FT-Raman spectral data of Spbzl.

Experimental wave numbers (cm^{-1})		Theoretical wave numbers (cm^{-1})		IR Intensity (au)	Raman Intensity (au)	Vibrational assignments (PED %)
FT-IR	FT-Raman	Scaled	Unscaled			
3000-2850		3545	3666.239	44	65	νNH(100)
		3134	3240.981	561	140	νOH(98)
	3061	3092	3197	17	232	νCH(90)
	2894	2933	3033	38	50	νCH(99)
1618	1617	1615	1670	250	1951	νNC(30), νCC(10),
1586	1599	1609	1664	22	203	νCC(43), νNC(10)
1582	1571	1585	1639	211	960	νCC(30)
1549		1564	1617	8	455	νCC(18)
1537	1536	1556	1609	234	2281	νNC(10), νCC(12)
	998	970	1004	11	228	τHCNC(66)
927		921	953	11	4	τHCCC(67)

ν and τ are stretching and torsion respectively.

3.3 ^{1}H and ^{13}C NMR Spectroscopic Studies

The ^{1}H and ^{13}C NMR spectra of Spbzl were recorded in deuterated dimethyl sulfoxide (DMSO-d6) and deuterated methanol (CD_3OD). The spectral data computed using hybrid model B3LYP/6-311G(d, p) are given in Tables 3 and 4. The experimental values are comparable with those reported for similar molecule [24]. The signals due to NH and OH protons are not observed in the ^{1}H NMR spectra recorded in CD_3OD, owing to deuterium exchange. The ring proton resonances are in the range δ 7.0-8.2 ppm. The azomethine proton resonance is observed as singlet at 8.9 ppm (CD_3OD) and 9.1 ppm (DMSO-d6). The OH resonance is observed at 12.8 ppm in DMSO-d6.

Table 3

^{1}H NMR experimental data and calculated values of Spbzl.

Proton number	δ in CD_3OD (ppm)*	δ in DMSO-d6 (ppm)*	δ using DFT (ppm)
4	7.3d(6)	7.2d(6)	8.0
5	7.6t(8)	7.6t(9)	7.6
6	7.6t(6)	7.6t(4)	7.6
7	7.2d(6)	7.2d(6)	7.8
2′	8.1s	8.2s	8.7
4′	7.5d(7)	7.5d(8)	7.5
5′	7.6t(8)	7.6t(10)	7.9
6′	8d(8)	8.1d(8)	7.9
3″	7d(8)	7d(8)	7.2
4″	7t(7)	7t(7)	7.7
5″	7.4t(8)	7.4t(8)	7.2
6″	7.5d(8)	7.7d(8)	7.8
N=C-H	8.9s	9.1s	8.8
Imine & OH	---	12.8s	12.8

*Coupling constants (Hz) are given in parentheses

Table 4
^{13}C NMR experimental and theoretical chemical shift values of Spbzl.

Carbon number	δ in CD_3OD (ppm)	δ in DMSO (ppm)	δ using DFT (ppm)
2	152.7	150.7	153.7
3′	150.9	148.3	158.9
2′	120.7	119.4	130.3
4′	124.1	122.5	126.0
2″	162.2	160.3	171.0
3″	117.9	119.2	122.4
4″	134.6	133.5	141.2
5″	115.5	116.6	124.5
6″	133.9	132.5	140.7
Azomethine	165.5	164.0	171.5

3.4 Photophysical Properties

The normalized UV-Vis absorption and fluorescence emission spectra of Spbzl showed the band edge position ($E_{0\text{-}0}$) at 364 nm (Fig. 5). The experimental and calculated absorption wavelengths using TD-DFT method are listed in Table 5. The calculated transition using B3LYP/6-311G(d, p) method corresponding to 332 nm is very strong with an oscillatory strength of 0.28. Using the CAM-B3LYP functional with 6-311G(d, p) basis set, the excitation wavelength was at 294 nm (Table 5) with oscillatory strength of 0.43 and is close to the experimental value 301 nm. The excitation wavelength determined using CAM-B3LYP for Pbzlb in DMF was at 274 nm (Table 5) with oscillatory strength 0.82.

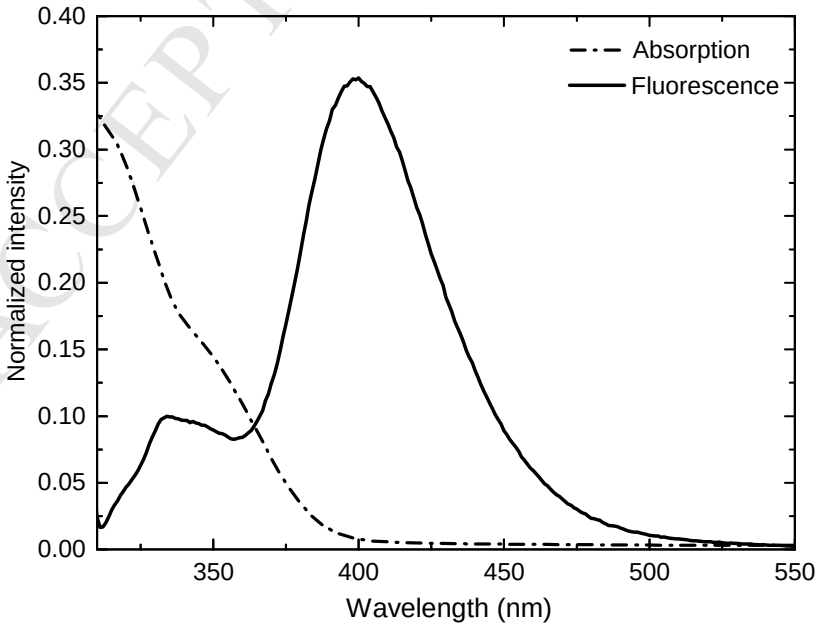

Fig. 5. Normalized UV absorption and fluorescence emission spectra of Spbzl in DMF.

Table 5
Optical and quantum chemical parameters.

Parameters	Values
λ_{abs}(max) (nm)	301
λ_{abs} (nm) by DFT	332[a], 294[a*], 274[b*]
E_{HOMO} (eV) by CV	–5.44
E_{LUMO} (eV) by CV	–2.03
E_{HOMO} (eV) by DFT	–6.03[a], –6.11[b]
E_{LUMO} (eV) by DFT	–2.04[a], –2.51[b]
Electronegativity, χ (eV)	4.03[a], 4.31[b]
Chemical hardness, η (eV)	1.99[a], 1.80[b]
Chemical potential, ρ (eV)	–4.03[a], –4.31[b]
Electrophilicity, ω (eV)	4.08[a], 5.16[b]

[a] -For Spbzl calculated using B3LYP functional; [a*]- For Spbzl calculated using CAM-B3LYP functional; [b] - For Pbzlb calculated using B3LYP functional; [b*]- For Pbzlb calculated using CAM-B3LYP functional.

3.5 Energy Level Analysis using Cyclic Voltammetry and DFT Studies

The charge transfer properties across the semiconductor dye interface in a dye sensitized solar cell will depend on the energy level of lowest unoccupied molecular orbital (LUMO) in the sensitizer such as Spbzl and the conduction band level of the semiconductor like TiO_2. The LUMO level of the sensitizer should be at a higher position than the conduction band of the semiconductor for better charge transfer. Effective regeneration of the dye from the electrolyte occurs when highest occupied molecular orbital (HOMO) energy level of the dye is below that of the electrolyte. In order to evaluate these properties for Spbzl, electrochemical measurements were carried out using cyclic voltammetry (CV). Fig. 6 shows CV curve for Spbzl.

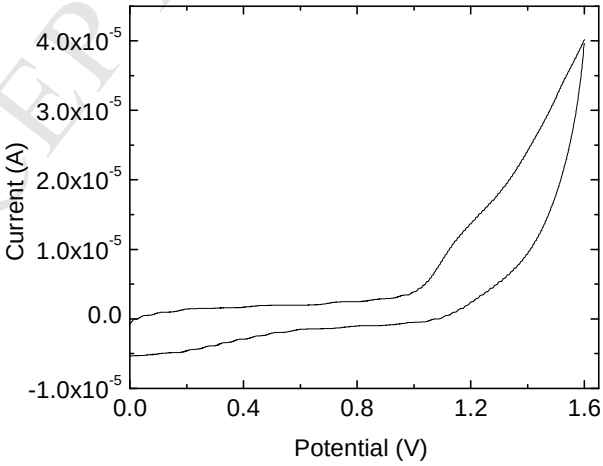

Fig. 6. Cyclic voltammetry curve.

HOMO energy level of the dye was obtained using onset oxidation potential (E_{ox}) 1.15 eV from CV curve with respect to reference energy value 4.8 eV [25] of ferrocene (Fc) using the equation (1),

$$E_{HOMO} = -(E_{ox} - E_{FC} + 4.8) \quad (1)$$

where E_{Fc} is the oxidation potential of ferrocene obtained to be 0.51 eV using the same experimental setup. Energy of LUMO level was obtained from equation (2),

$$E_{LUMO} = E_{HOMO} + E_{0-0} \quad (2)$$

Here $E_{0\text{-}0}$ is the onset energy, whose value obtained from absorption and emission spectra (Fig. 5) is 3.41 eV. Experimental E_{HOMO} and E_{LUMO} values are comparable with the theoretical values obtained from DFT (Table 5). The E_{LUMO} of Spbzl (−2.03 eV) is well above the conduction band of TiO_2 (−4 eV) [26] indicating that the charge from excited sensitizer can be easily driven to TiO_2 [27]. It is also clear that the E_{HOMO} level (−5.44 eV) of the dye is below the HOMO level of electrolyte (I^-/I_3^-) −4.6 eV [28] signifying the effective regeneration of the dye from electrolyte (Fig. 7). The computational values of HOMO and LUMO for Pbzlb were obtained at −6.11 eV and −2.51 eV respectively. This shows that the substitution of COOH group at para position (for Pbzlb) has reduced the energy gap from 4.0 eV to 3.60 eV. Frontier molecular orbital analysis was carried out to understand the charge transfer during oxidation from donor to acceptor moiety of the molecule (Fig. 7). It is observed that the electron density is concentrated on benzimidazole ring (donor) on HOMO surface and charge transfer has taken place from benzimidazole to π-bridge and salicylidene ring (acceptor) in LUMO level. For Pbzlb, the charge has been distributed on salicylidene ring extending to COOH unit (Fig. 7). This shows that the charge transfer from Pbzlb to the semiconductor surface in DSSC is feasible.

The chemical potential is an indication of diffusion of atoms from higher potential to lower potential and is located in the energy gap between HOMO and LUMO. The chemical potential (ρ) −4.03 eV (Table 5) for Spbzl is close to −4.02 eV obtained for YD2-o-C8 [27] which is considered as a good sensitizer. Chemical potential (ρ) value for Pbzlb is −4.31 eV. Better intramolecular charge transfer is evidenced by the lower value of chemical hardness (η), the value −1.99 eV for Spbzl is found to be lower compared to −2.13 eV of YD2-o-C8 (−1.80 eV for Pbzlb) indicating better ICT in Pbzlb compared to Spbzl. The electrophilicity indices (ω) for Spbzl and Pbzlb obtained from DFT computations are 4.08 eV and 5.16 eV which is higher compared to 3.79 eV for YD2-o-C8. This is an indication of good stability and electron withdrawing nature of Pbzlb compared to Spbzl which can improve the photovoltaic performance.

3.6 Natural Bonding Orbital (NBO) Analysis

The delocalization of electrons from Lewis (donor) orbital to non-Lewis (acceptor) orbital leads to the stabilization of the system. This donor-acceptor interaction can be quantized based on the stabilization energy (E2) calculated using second order perturbation theory

analysis of Fock-matrix in NBO. Higher the stabilization energy greater is the interaction between donor and acceptor orbitals. Stabilization energy values considered here are more than the standard threshold value of 20.63 kJ mol^{-1}. The stabilization energies due to the intramolecular charge transfer (ICT) leading to the stabilization of Spbzl are calculated to be 84.39 kJ mol^{-1} due to the interaction between π (C15-C16) and π* (C20-C19) as well as π (C12-C11) and π* (C10-C9), 84.61 kJ mol^{-1} due to the interaction between π (C10-C9) and π* (C13-C8) and 91.86 kJ mol^{-1} due to the interaction between π (C6-C1) and π* (C5-C4) orbitals. Further details on the stabilization energies and donor-acceptor interactions existing in the molecule are given as supplementary information (STable 3).

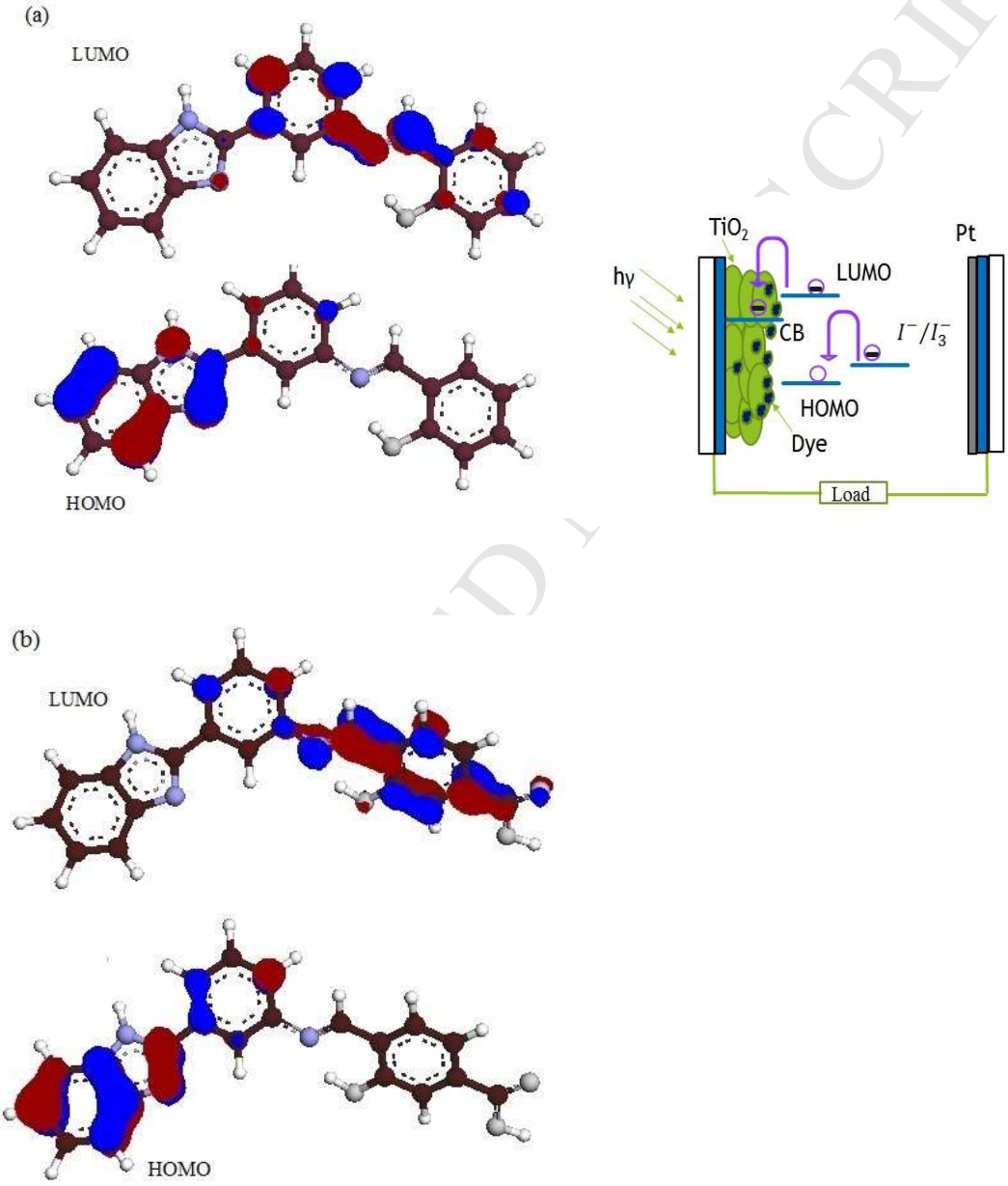

Fig. 7. Charge distribution on LUMO and HOMO surfaces of (a) Spbzl and (b) Pbzlb.

3.7 Nonlinear Optical (NLO) Studies

NLO properties of Spbzl were determined in gas and solution (dichloromethane; DCM) phases using B3LYP/6-311G(d, p) method. The parameters such as mean polarizability (Δα), dipole moment (μ) and mean first hyperpolarizability (β) based on x, y, z components were calculated according to equations (3), (4) and (5) respectively [29],

$$\Delta\alpha = 2^{-1/2}\left[\left(\alpha_{xx}-\alpha_{yy}\right)^2+\left(\alpha_{yy}-\alpha_{zz}\right)^2+(\alpha_{zz}-\alpha_{xx})^2+6\alpha_{xx}^2\right]^{1/2} \quad (3)$$

$$\mu = \left(\mu_x^2+\mu_y^2+\mu_z^2\right)^{1/2} \quad (4)$$

$$\beta = \left(\beta_x^2+\beta_y^2+\beta_z^2\right)^{1/2} \quad (5)$$

The mean polarizability Δα calculated (Table 6) using equation (3) for Spbzl in DCM (8.70×10^{-30} esu) is higher compared to that in gas phase (6.95×10^{-30} esu). This implies that the molecule is interacting with the surrounding environment [30] and also there is significant charge transfer among the molecules. This variation is also supported by the solvatochromic studies [19]. The dipole moment (μ) and the mean first hyperpolarizability (β) values were calculated using equations (4) and (5) respectively (Table 6). The higher dipole moment (3.02 D) in solution phase as compared to in gas phase (2.11 D) indicates an increased intramolecular charge transfer in solution. The mean first hyperpolarizability values obtained from B3LYP method for Spbzl in gas (1.27×10^{-29} esu) and solution (DCM) phases (2.19×10^{-29} esu) are higher than that for urea (9.13×10^{-31} esu in gas) and (10.3×10^{-31} esu in DCM). It is reported that B3LYP method overestimates the NLO parameters due to the poor accountancy of electron exchange interaction [31] and the long range order corrected functional CAM-B3LYP (which incorporates HF exchange functional along with the hybrid exchange functional) gives better estimate for these NLO parameters [32]. Hence we also computed NLO parameters using CAM-B3LYP functional in gaseous and solution phase for urea, Spbzl and Pbzlb molecules (Table 6). Mean first hyperpolarizability using CAM-B3LYP in gaseous state and in DCM for both Spbzl and urea (7.15×10^{-31} esu in gas and 7.98×10^{-31} esu in DCM) has been reduced compared to that obtained using B3LYP functional. The NLO parameters computed using CAM-B3LYP for Pbzlb are higher compared to Spbzl (Table 6).

The high value of mean first hyperpolarizability from calculation prompted us to measure the second harmonic generation (SHG) efficiency using Kurtz-Perry method and compare with that of KDP and urea. The SHG efficiency was measured using Q-switched Nd:YAG laser. The powder sample filled in a capillary tube was subjected to a beam of wavelength 1064 nm. The input energy of 1.2 mJ $pulse^{-1}$ with repetition rate of 10 nHz and pulse width of 10 ns was used. The monochromatic second harmonic signal was measured using photomultiplier tube. The SHG efficiency was found to be 3% (1.3 mV) of the value of urea (42 mV) and 22% of the value of KDP (6 mV). Though the computed mean first hyperpolarizability values were high compared to urea, the experimental NLO efficiency is negligible. However a direct comparison between computed values and experimental values

cannot be made as the NLO parameters are obtained at non-zero frequencies unlike computational ones measured at zero frequency [33].

Table 6
Nonlinear optical parameters

Parameters	Values
Mean polarizability in gas phase, Δα (au)	804[a], 724[a*], 834[b*]
Mean polarizability in gas phase, Δα (esu)	6.95×10^{-30} [a], 1.07×10^{-22} [a*], 1.24×10^{-22} [b*]
Mean polarizability in DCM, Δα (au)	1007[a], 882[a*], 1008[b*]
Mean polarizability in DCM, Δα (esu)	8.70×10^{-30} [a], 1.31×10^{-22} [a*], 1.49×10^{-22} [b*]
Dipole moment in gas phase, μ (D)	2.11[a], 1.85[a*], 2.04[b*]
Dipole moment in DCM, μ (D)	3.02[a], 2.57[a*], 2.80[b*]
Mean first hyperpolarizability in gas phase, β (au)	1469[a], 982[a*], 1710[b*]
Mean first hyperpolarizability in gas phase, β (esu)	1.27×10^{-29} [a], 0.85×10^{-29} [a*], 1.48×10^{-29} [b*]
Mean first hyperpolarizability in DCM, β (au)	2534[a], 1586[a*], 3022[b*]
Mean first hyperpolarizability in DCM, β (esu)	2.19×10^{-29} [a], 1.37×10^{-29} [a*], 2.61×10^{-29} [b*]

[a]- For Spbzl calculated using B3LYP functional; [a*] - For Spbzl calculated using CAM-B3LYP functional; [b*]- For Pbzlb calculated using CAM-B3LYP functional.

4. Conclusions

X-ray single crystal studies on Spbzl have revealed the presence of two water molecules in the asymmetry unit. The crystal packing is stabilized by the intermolecular interactions aided through water molecules. The C-C, C-O, C-N and C=N bond lengths suggest the presence of intramolecular charge transfer in Spbzl. This is also supported by NBO analysis carried out using DFT. Experimental results of NMR, FT-IR and FT-Raman spectra are supported by theoretical data obtained using DFT. The higher E_{LUMO} value of Spbzl compared to conduction band edge of TiO_2 semiconductor suggests that there is sufficient driving force for an electron to be transferred from the sensitizer to the semiconductor. The lower E_{HOMO} compared to that of electrolyte (I^-/I_3^-) is suitable for effective regeneration of the dye from electrolyte. HOMO and LUMO surface analysis on Spbzl and Pbzlb indicates that the charge transfer takes place from benzimidazole to salycilidene moiety in both the molecules. Also feasibility of charge transfer from sensitizer to semiconductor is more in Pbzlb compared to Spbzl. Based on these it is expected that Spbzl can be further tuned for dye sensitized solar cell studies.

References

[1] P. N. Preston, The chemistry of heterocyclic compounds, benzimidazoles and congeneric tricyclic compounds, John-Wiley and Son, New York (1980).

[2] J. Li, Q. Hu, X. Yu, Y. Zeng, C. Cao, X. Liu, J. Guo, Z. Pan, A novel rhodamine-benzimidazole conjugate as a highly selective turn-on fluorescent probe for Fe^{3+}, J. Fluoresc. 21 (2011) 2005-2013.

[3] J. Kulhanek, F. Bures, Imidazole as a parent π-conjugated backbone in charge-transfer chromophores, J. Org. Chem. 8, (2012) 25-49.

[4] S. Y. Takizawa, V. A. Montes, P. Anzenbacher, Phenylbenzimidazole-based new bipolar host materials for efficient phosphorescent organic light-emitting diodes, Chem. Mater. 21 (2009) 2452-2458.

[5] M. Liang, J. Chen, Arylamine organic dyes for dye-sensitized solar cells, Chem. Soc. Rev. 42 (2013) 3453-3488.

[6] D. Vlaovic, J. C. Brunet, J. Balaz, I. Juranic, D. Djokovic, K. Mackenzie, Synthesis, antibacteriol, and antifungal activities of some new benzimidazoles, Biosci. Biotech. Biochem. 56 (1992) 199-206.

[7] H. Durr, Perspectives in photochromism: A novel system based on the 1,5-electrocyclization of heteroanalogous pentadienyl anions, Angew. Chem. Int. Ed. 28 (1989) 413-431.

[8] H. Durr, H. Bouas-Laurent, Photochromism molecules and systems, Elsevier, Amsterdam, (1990).

[9] E. Hadjoudis, I. M. Mavridis, Photochromism and thermochromism of Schiff bases in the solid state: structural aspects, Chem. Soc. Rev. 33 (2004) 579-588.

[10] X. Zhang, Y. Zhu, X. Wu, H. He, G. Wang, Q. Li, Meso-Schiff-base substituted porphyrin dimer dyes for dye-sensitized solar cells: synthesis, electrochemical, and photovoltaic properties, Res. Chem. Intermed. 41 (2015) 4227-4241.

[11] Q. Tan, X. Zhang, L. Mao, G. Xin, S. Zhang, Novel zinc porphyrin sensitizers for dye-sensitized solar cells: Synthesis and spectral, electrochemical, and photovoltaic properties, J. Mol. Struct. 1035 (2013) 400-406.

[12] Y. H. Wu, L. Chen, J. Yu, S. L. Tong, Y. Yan, Synthesis and spectroscopic characterization of meso-tetra (Schiff-base substituted phenyl) porphyrins and their zinc complexes, Dyes Pigments 97 (2013) 423-428.

[13] B. Roopashree, V. Gayathri, A. Gopi, K. S. Devaraju, Syntheses, characterizations, and antimicrobial activities of binuclear ruthenium(III) complexes containing 2-substituted benzimidazole derivatives, J. Coord. Chem. 65 (2012) 4023-4040.

[14] M. J. Frisch, G. W. Trucks, H. B. Schlegel, G. E. Scuseria, M. A. Robb, J. R. Cheeseman, G. Scalmani et al. Gaussian 09, Revision E.01, Gaussian, Inc., Wallingford CT (2009).

[15] L. Zhang, J. M. Cole, P. G. Waddell, K. S. Low, Xiaogang Liu, Relating electron donor and carboxylic acid anchoring substitution effects in azo dyes to dye-sensitized solar cell performance, ACS Sustainable Chem. Eng. 1 (2013) 1440–1452.

[16] J. Rochford, D. Chu, A. Hagfeldt, E. Galoppini, Tetrachelate porphyrin chromophores for metal oxide semiconductor sensitization: effect of the spacer length and anchoring group position, J. Am. Chem. Soc. 129 (2007) 4655-4665.

[17] A. S. Hart, B. K. C. Chandra, B. G. Habtom, L. R. Sequeira, F. D'Souza, Porphyrin-Sensitized Solar Cells: Effect of Carboxyl Anchor Group Orientation on the Cell Performance, ACS Appl. Mater. Interfaces 5 (2013) 5314‑5323.

[18] G. M. Sheldrick, SHELX-97 University of Gottingen Germany (1997).

[19] G. R. Suman, S. G. Bubbly, S. B. Gudennavar, J. Thipperudrappa, B. Roopashree, V. Gayathri, N. M. Nanje Gowda, Effect of solvents on photophysical properties and quenching of 2-{[3-(1H-benzimidazole-2-yl) phenyl] carbonoimidoyl}phenol, Luminescence 30 (2015) 611-618.

[20] A. D. Becke, Density-functional thermochemistry. III. The role of exact exchange, J. Chem. Phys. 98 (1993) 5648-5652.

[21] C. Lee, W. Yang, R. G. Parr, Development of the Colle-Salvetti correlation-energy formula into a functional of the electron density, Phys. Rev. B37 (1998) 785-789.

[22] J. A. Pople, A. P. Scott, M. W. Wong, L. Radom, Scaling factors for obtaining fundamental vibrational frequencies and zero-point energies from HF/6–31G* and MP2/6–31G* harmonic frequencies, Isr. J. Chem. 33 (1993) 345-350.

[23] M. Chandrakala, B. S. Sheshadri, N. M. Nanje Gowda, K. G. S Murthy, K. R. Nagasundara, Synthesis and spectral studies of 2-salicylidine-4-aminophenyl benzimidazole and its reaction with divalent Zn, Cd and Hg: crystal structure of the cadmium bromide complex, J. Chem. Res. 10 (2010) 576-580

[24] M. Chandrakala, N. M. Nanje Gowda, K. G. S. Murthy, K. R. Nagasundara, Activation of – N=CH – bond in a Schiff base by divalent nickel monitored by NMR evidence, Magn. Reson. Chem. 50 (2012) 335-340.

[25] J. Pommerehne, H. Vestweber, W. Guss, R. F. Mahrt, H. Bässler, M. Porsch, J. Daub, Efficient two layer LEDs on a polymer blend basis, Adv. Mater. 7 (1995) 551-554.

[26] M. Gratzel, Photoelectrochemical cells, Nature 414 (2001) 338-344.

[27] K. Chaitanya, X. H. Ju, B. M. Heron, Theoretical study on the light harvesting efficiency of zinc porphyrin sensitizers for DSSCs, RSC. Adv. 4 (2014) 26621-26634.

[28] G. Boschloo, A. Hagfeldt, Characteristics of the iodide/triiodide redox mediator in dye-sensitized solar cells, Acc. Chem. Res. 42 (2009) 1819-1826.

[29] N. Swarnalatha, S. Gunasekaran, S. Muthu, M. Nagarajan, Molecular structure analysis and spectroscopic characterization of 9-methoxy-2H-furo[3,2-g]chromen-2-one with

experimental (FT-IR and FT-Raman) techniques and quantum chemical calculations Spectrochim. Acta Mol. Biomol. Spectrosc. 137 (2015) 721-729.

[30] J. I. Nishida, T. Masuko, Y. Cui, K. Hara, H. Shibuya, M. Ihara, T. Hosoyama, R. Goto, S. Mori, Y. Yamashita, Molecular design of organic dye toward retardation of charge recombination at semiconductor/dye/electrolyte interface: Introduction of twisted π-Linker, J. Phys. Chem. C 114 (2010) 17920-17925.

[31] M. D. Wergifosse, B Champagne, Electron correlation effects on the first hyperpolarizability of push–pull π-conjugated Systems, J. Chem. Phys. 134 (2011) 074113(1-13).

[32] S. N. Margar, N. Sekar, Nonlinear optical properties of curcumin: solvatochromism-based approach and computational study, Molecul. Phys. (2016) 1867-1879.

[33] Y. Dai, Z. Li, J. Yang, Density functional study of nonlinear optical properties of grossly warped nanographene C80H30, J. Phys. Chem. C 118 (2014) 3313-3318.

Highlights:

- Crystal structure of the Schiff base Spbzl has been solved using single crystal XRD.
- Experimental spectroscopic data (FT-IR, Raman and NMR), photophysical properties and energy level values are compared with the theoretical ones obtained using DFT.
- CAM-B3LYP method used to compare photophysical properties and charge distribution in Spbzl and its derivative having COOH anchoring group.
- NLO measurements carried out for Spbzl using Kurtz-Perry setup and NLO parameters obtained using DFT method.